Push recovery for the standing under-actuated bipedal robot using the hip strategy[*]

Chao LI, Rong XIONG[†‡], Qiu-guo ZHU, Jun WU, Ya-liang WANG, Yi-ming HUANG

(*State Key Laboratory of Industrial Control Technology & Institute of Cyber-Systems and Control,*

Zhejiang University, Hangzhou 310027, China)

[†]E-mail: rxiong@iipc.zju.edu.cn

Abstract: This paper presents a control algorithm for push recovery, which particularly focuses on the hip strategy when an external disturbance is applied on the body of a standing under-actuated biped. By analyzing a simplified dynamic model of a bipedal robot in the stance phase, it is found that horizontal stability can be maintained with a suitably controlled torque applied at the hip. However, errors in the angle or angular velocity of body posture may appear, due to the dynamic coupling of the translational and rotational motions. To solve this problem, different hip strategies are discussed for two cases when (1) external disturbance is applied on the center of mass (CoM) and (2) external torque is acting around the CoM, and a universal hip strategy is derived for most disturbances. Moreover, three torque primitives for the hip, depending on the type of disturbance, are designed to achieve translational and rotational balance recovery simultaneously. Compared with closed-loop control, the advantage of the open-loop methods of torque primitives lies in rapid response and reasonable performance. Finally, simulation studies of the push recovery of a bipedal robot are presented to demonstrate the effectiveness of the proposed methods.

1 Introduction

The push recovery capability of a bipedal robot under unexpected external disturbance during standing is essential for real-world applications in the human environment. Originally designed tasks, such as standing or walking, would inevitably be affected by some unexpected perturbations, such as collisions with obstacles or interaction with people. To avoid falling and achieve better walking performance, a class of controllers must be developed to maintain balance and recover upright posture for bipedal robots.

Humans often use two strategies to maintain balance during standing, depending on the amount of external force applied to the body (Horak and Nashner, 1986; Runge *et al.*, 1999; Azevedo *et al.*, 2007). One is the ankle strategy, where all the joints above the ankle are fixed and thus all the links are considered as one rigid body, and the ankle torque is used to counteract small perturbations. The other is the hip strategy, where hip torque is used to rotate the body and control the center of mass (CoM) for large perturbations. The above two strategies can work together to maintain balance. For large and rapid perturbations of a certain size and speed, a stepping strategy must be adopted since a biped physically could not withstand the disturbance (Horak and Nashner, 1986; Azevedo *et al.*, 2007).

For bipedal robots, the same ankle and hip strategies have been employed for standing balance control (Pratt *et al.*, 2006; Stephens, 2007a; 2007b). However, balance control is often at the expense of

posture errors due to the coupling effects in the translational and rotational dynamics of the body. The optimal solution would be one where push recovery does not affect the original upright posture. Therefore, we aim at a push recovery that can achieve rotational and translational balance simultaneously, since most of the external disturbances would influence both attitude and position of the body.

The algorithms proposed in this paper attempt to achieve both CoM position control and upper body attitude control during push recovery for bipedal robots during standing using only the hip strategy. In other words, we seek a hip strategy that achieves balance recovery of the CoM position of body orientation with no involvement of the ankle, i.e., point feet. If this can be done with this algorithm, then an even better performance can be achieved by adding feet to introduce ankle torque as an additional control. First, we point out that the goal of balance control is to make the horizontal position of the CoM converge back to a stable orbit based on the motion analysis of the bipedal robot in a standing phase. External disturbances are classified into three cases according to their influence, and we examine three corresponding control methods which are named symmetrical bang-bang-bang (STB), asymmetrical bang-bang-bang (ATB), and universal bang-bang-bang (UTB) control. STB control can restore the balance in horizontal motion without affecting the initial upright posture. ATB control can recover an upright posture or redirect the body to any orientation without degrading its balance. UTB control can regulate CoM position control and body orientation control simultaneously.

Compared with closed-loop control, the above open-loop methods of torque primitives serve more like a reflex control, being fast and rapid. However, in practice, due to the errors in modeling, the balance of the bipedal robot controlled only by the open-loop methods will be eventually lost, and thus a closed-loop control would also be required to generate fine modulation after open-loop control. Hence, the proposed torque primitives can be regarded as a torque reflex control to achieve a fast reaction to the unexpected impulsive perturbation, while closed-loop control may be involved in a later stage. Logically, an optimal solution should combine the merits of the open-loop torque primitive and closed-loop control into one framework. Usually some simple closed-loop control, e.g., linear quadratic regulator (LQR) control, for push recovery can be easily achieved. Thus, this paper focuses on open-loop methods of torque primitives.

2 Related work

For bipedal robots, Pratt *et al.* (2006) demonstrated a simple and effective bang-bang profile for hip torque, which can be used to restore the horizontal equilibrium into stable regions, but at the expense of a body posture error. Stephens (2007a) solved this problem using optimal control for the linearized system where torques of hip and ankle are both control variables, and LQRs were designed for simultaneous balance control and posture recovery during standing. Later, he presented integral control, by which smooth torque references were generated by decoupling the dynamics of horizontal motion and body posture, allowing a bipedal robot to recover balance from large disturbances and at the same time maintain an upright posture (Stephens, 2007b). Stephens and Atkeson (2010) further presented a dynamic balance force control method for determining full body joint torques based on the desired CoM motion and contact forces for compliant humanoid robots. Whitman *et al.* (2012) presented a modification for a broad class of controllers based on linear inverted pendulum model (LIPM) dynamics. Instead of controlling the CoM, an 'augmented center of mass', which was unaffected by angular accelerations of upper body, was controlled. An improved robustness to external pushes with this control method was demonstrated through simulations and experiments on a force-controlled humanoid robot. Liu and Atkeson (2009) employed a library of optimal trajectories and the neighboring optimal control method to generate local approximations to the optimal control for standing balance control. Wang (2012) addressed the problem of dynamic stabilization and push recovery for humanoid robots using robust control through convex optimization. Li *et al.* (2012) employed three compliance controllers in the transversal plane, body attitude, and potential energy shaping respectively, for standing maintenance. The experiments conducted on the compliant humanoid robot COMAN showed that the robot can recover from external impacts and adapt to slopes and

uneven grounds. Wang *et al.* (2014) designed a controller with variable gains based on a virtual model to generate the desired recovery forces and an admittance controller for a position-controlled robot to achieve the compliant control for the standing maintenance under unknown disturbances.

Some researchers have attempted to maintain standing balance by controlling the ground reaction forces or using the momentum-based controller. Hyon *et al.* (2007) presented a balance controller that transforms the required ground reaction force into the full-body joint torques, which enable the compliant humanoid robot to stand stably under disturbance from unknown external forces. Lee and Goswami (2010) presented a momentum-based method for maintaining balance of bipedal robots by controlling the desired ground reaction forces and center of pressure at each support foot. Orin *et al.* (2013) studied the properties, structure, and computation schemes for the centroidal momentum matrix (CMM) and introduced a concept of 'average spatial velocity' of the humanoid that encompasses both linear and angular components and provides a novel decomposition of the kinetic energy. A momentum-based balance controller that directly employs the CMM can significantly reduce unnecessary trunk bending during balance maintenance against external disturbance.

The aforementioned methods for balance control and push recovery require coordination between hip and ankle joints, instead of controlling only the hip joint. However, for some bipeds and one-legged robots without feet, these methods are no longer valid, or are significantly downgraded due to the lack of an ankle joint. Some past studies have addressed the same issue by controlling only the hip. The balance control using only the hip strategy for a bipedal robot is similar to the stability control for a two-link acrobot, where the hip torque is controlled and the ankle is unactuated (Spong, 1995). The acrobot uses the hip torque to generate the horizontal ground forces which keep the CoM above the foot. The acrobot system has been proved stable and can maintain balance. Referring to balance control of the acrobot, Ahmed *et al.* (2013) presented a nonlinear control for the stabilization of standing posture for a bipedal robot using only the hip joint. The robot is modeled as an acrobot and the model parameters are estimated through an adaptive algorithm. The evaluation in the Webots

simulator and experiments on a physical humanoid robot, NUSBIP-III ASLAN, verify the effectiveness of the proposed method.

We focus on the hip strategy and intend to achieve the same control performance for both the CoM and the body attitude using only the hip torque. This paper begins with a biped model with point feet and thus no ankle joint. By analyzing only the stance phase and the dynamic characteristics of the model, we find that the hip torque can be used to recover the balance of the robot. Mathematically, we attempt to use the one degree of freedom (DoF) at the hip to control two target variables, the CoM state and the body attitude. However, due to the dynamic coupling of the translational and rotational movements, the body attitude error will inevitably occur if only the control of CoM in the horizontal plane is applied. To solve this problem, we classify the external disturbances acting on the robot into three cases, and therefore three different hip torque primitives are designed, depending on the case of disturbances.

3 Modeling of an under-actuated bipedal robot

3.1 Dynamic equations of a bipedal robot in the stance phase

In this study, we use a simplified biped model as shown in Fig.1a. The simplified biped is a rigid body that represents the mass and inertia of the whole robot, and has a two-link leg which consists of two segments concatenated by a knee joint. The hip joint is located at the center of the body. Since there is no ankle joint, balance control can be achieved only by a controller supplying hip torque. The contact point between the shank and ground can be considered as an imaginary ankle joint which is under-actuated (zero torque) for the convenience of the following analysis and discussion. This bipedal model will also be used in the following simulation study.

To simplify the dynamic analysis of the bipedal robot as shown in Fig. 1a, we provide an equivalent linear inverted pendulum plus flywheel model (LIPFM) as shown in Fig. 1b. The motion of the body depends on three equivalent forces/torques applied on the rigid body. Equivalent joint torques of the stance leg can be obtained using the force Jacobian matrix:

$$
\begin{bmatrix} \tau_a \\ \tau_k \\ \tau_h \end{bmatrix} = \begin{bmatrix} z & -x & 1 \\ l_2 \cos(\theta_a + \theta_k) & -l_2 \sin(\theta_a + \theta_k) & 1 \\ 0 & 0 & 1 \end{bmatrix} \begin{bmatrix} F_x \\ F_z \\ \tau_b \end{bmatrix},
\tag{1}
$$

where F_x, F_z, and τ_b are virtual horizontal force, vertical force, and torque imposed on the CoM by the virtual leg, respectively. τ_a, τ_k, and τ_h are equivalent joint torques of the ankle, knee, and hip, respectively. x and z are the horizontal and vertical positions of the CoM, respectively. θ_a and θ_k are the angles of the ankle and knee, respectively. l_2 is the length of the upper leg.
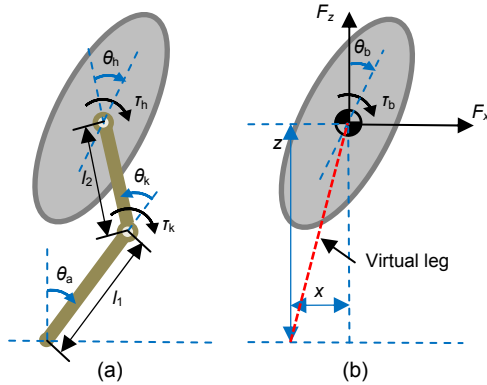

Fig. 1 The simplified model of a bipedal robot (a) and the equivalent linear inverted pendulum plus flywheel model (LIPFM) (b)
In (a), the hip and knee joints are located at the body center (also the CoM of the body) and between the leg segments, respectively; In (b), three equivalent forces/torques applied by the virtual leg are imposed on the CoM

Because the imaginary ankle joint is underactuated, the torque of ankle remains zero. Substituting the constraint $\tau_a=0$ into the first line of Eq. (1), we can obtain the internal constraint of the three virtual forces/torques:

$$
F_x = \frac{x}{z} F_z - \frac{\tau_h}{z}.
\tag{2}
$$

Assuming the vertical motion of the CoM is constrained on a horizontal plane, the vertical acceleration is zero. Hence, we have $F_z=mg$, where m is the mass of the body and g the gravitational acceleration.

According to the last line of Eq. (1), i.e., $\tau_b=\tau_h$, and substituting F_z and τ_h into Eq. (2), we obtain the horizontal motion equation of the body:

$$
\ddot{x} = \omega^2 x - \frac{\tau_h}{zm},
\tag{3}
$$

where $\omega = \sqrt{g/z}$. Meanwhile, the rotation motion equation of the body imposed by hip torque is

$$
\ddot{\theta}_b = \frac{\tau_h}{J},
\tag{4}
$$

where J is the inertia tensor of the body around the CoM.

Define the control target of simultaneous balance and posture control as follows:

1. Horizontal position and velocity are both 0 ($x=0$, $\dot{x}=0$), which is also called 'rest state'.

2. Angle and angular velocity of the body are both 0 ($\theta_b=0$, $\dot{\theta}_b=0$), which is also called 'upright posture'.

3.2 Stable orbit of balance control

By setting $\tau_h=0$, the LIPFM is equal to the LIPM. We introduce a quantity called 'LIPM orbital energy' (Kajita and Tani, 1991), which is conserved if no external energy is injected into the system:

$$
E_{LIPM} = \frac{1}{2}\dot{x}^2 - \frac{1}{2}(\omega x)^2.
\tag{5}
$$

The body would slow down and finally stop at the rest state only when $E_{LIPM}=0$. There are two different eigenvectors, i.e., $\dot{x}=\pm\omega x$, and $\dot{x}=-\omega x$ is the only stable eigenvector (Pratt *et al.*, 2006). Then define a variable named 'stable offset' to determine whether or not the horizontal motion is stable:

$$
S = \omega x + \dot{x}.
\tag{6}
$$

When $S=0$, the horizontal motion is stable; otherwise, it is unstable. The phase portrait x is established to describe the state of the horizontal motion with x and $\dot{x}$ as its abscissa and ordinate, respectively. In the phase portrait, we find that all the states which satisfy $S=0$ form a line, defined as the 'stable orbit' in this study. All states in the stable orbit are defined as stable states. If the state is not on the stable orbit, the robots will pass over or cannot reach the rest state, and $|x|$ and $|\dot{x}|$ will diverge to infinity. Due to the

limits of the friction cone or the joint angle, the robot will eventually fall.

Based on the above analysis, we can obtain equivalent control targets:

$$\begin{cases} S = 0, \\ \theta_b = 0, \\ \dot{\theta}_b = 0. \end{cases} \quad (7)$$

According to Eq. (3), E_{LIPM} can be influenced by the hip torque. In other words, there exists a solution of desired hip torque to control the horizontal motion of the robot.

3.3 Theoretically allowed stability threshold

A bipedal robot in the rest state will lose balance if an external force is pushing on its CoM. Assuming the horizontal position and velocity of the CoM after disturbance being x_0 and $\dot{x}_0$, respectively, substituting x_0 and $\dot{x}_0$ into Eq. (6) yields the initial stable offset caused by the disturbance:

$$S_0 = \omega x_0 + \dot{x}_0. \quad (8)$$

Regardless of the limits of the angle and angular velocity of the hip joint, we impose a maximum hip torque on the CoM to verify whether or not the horizontal motion can return to the stable orbit. The hip torque primitive is defined as follows:

$$\tau_M(t) = \text{sgn}(S_0) \cdot \tau_{\max}[1(t) - 1(t-T)], \quad (9)$$

where $\tau_{\max}$ is the maximum torque that the hip joint can apply, $1(t-T_*)$ is the unit step function starting at T_*, T is the duration of $\tau_M(t)$, and sgn() is the sign function.

Substituting $\tau_M(t)$ into Eq. (3) and solving the differential equations, we can obtain the horizontal position and velocity of the CoM at T:

$$\begin{bmatrix} x_M(T) \\ \dot{x}_M(T) \end{bmatrix} = \begin{bmatrix} \cosh(\omega T) & \dfrac{\sinh(\omega T)}{\omega} \\ \omega \sinh(\omega T) & \cosh(\omega T) \end{bmatrix} \begin{bmatrix} x_0 \\ \dot{x}_0 \end{bmatrix} \\ + \text{sgn}(S_0) \begin{bmatrix} \dfrac{\Phi}{\omega}[\cosh(\omega T) - 1] \\ \Phi \sinh(\omega T) \end{bmatrix}, \quad (10)$$

where $\Phi = \tau_{\max}/(mz_0\omega)$, with z_0 being the height of the CoM.

Substituting $x_M(T)$ and $\dot{x}_M(T)$ into Eq. (6), we obtain the stable offset at T:

$$S_M(T) = [S_0 - \text{sgn}(S_0) \cdot \Phi]e^{\omega T} + \text{sgn}(S_0) \cdot \Phi. \quad (11)$$

Taking the derivative of Eq. (11), we have

$$\dot{S}_M(T) = [S_0 - \text{sgn}(S_0) \cdot \Phi]\omega e^{\omega T}. \quad (12)$$

When $S_0 > \Phi$, we have $S_M(0) = S_0 > 0$ in Eq. (11) and $\dot{S}_M(T) = (S_0 - \Phi)\omega e^{\omega T} \geq (S_0 - \Phi)\omega > 0$ in Eq. (12) (due to $\omega T > 0$); $S_M(T)$ is always greater than 0 no matter what the value of T is. When $S_0 \leq -\Phi$, we have $S_M(0) < 0$ in Eq. (11) and $\dot{S}_M(T) = (S_0 + \Phi)\omega e^{\omega T} \leq (S_0 + \Phi)\omega < 0$ in Eq. (12); $S_M(T)$ is always less than 0. In these two cases, the balance of the bipedal robot can never be recovered. Regardless of the limits of the angle and angular velocity of the body, the theoretically allowed stability threshold is Φ, and thus all the allowable stable offsets should satisfy

$$|S_0| < \Phi. \quad (13)$$

Ideally, as long as the stable offset satisfies inequality (13), the balance can be recovered (proved in Section 4.1). However, in reality, due to the limits of the angle and angular velocity of the body, and the friction cone, the stability threshold becomes much smaller than Φ. As for the case in which the stable offset is greater than Φ, the stepping strategy should be adopted, which is beyond the scope of this study.

In fact, according to Eqs. (3) and (4), the hip torque not only changes the horizontal motion, but also affects the rotational motion of the body. Therefore, coupling errors may appear in the angular position and velocity of the body when balance control is being applied. So, a correct hip torque primitive should be designed to restore balance and upright posture at the same time.

4 Simultaneous balance control and posture recovery

In this section, we will introduce a novel strategy to control the hip torque which can restore the bipedal

robot standing balance and upright posture simultaneously. To begin with, we first discuss two special cases categorized by the way the external force/torque acts on the robot during standing: (1) The external force passes through the CoM which changes only the horizontal motion, without affecting the body posture (Fig. 2a); (2) The external torque applies on the CoM which changes only the body posture, without affecting the horizontal motion (Fig. 2b). Two effective torque primitives for the hip are designed particularly for each case. Based on this discussion, at the end of this section, we introduce a novel hip torque primitive for more universal cases, such as the case where the external force misaligns with the CoM and thus changes both horizontal motion and body posture (Fig. 2c).
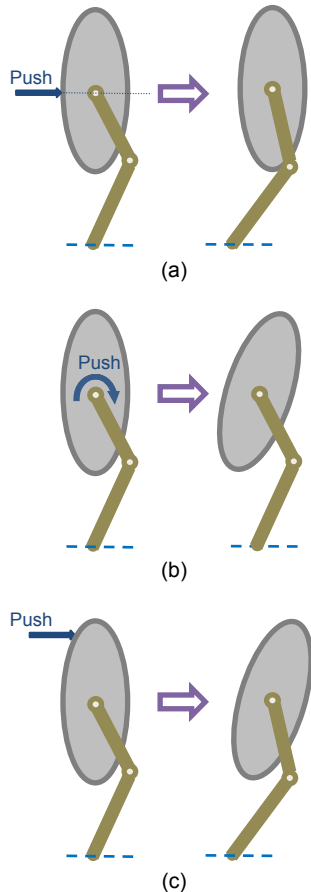
Fig. 2 Three different types of external force/torque disturbances
(a) External force passes through the CoM; (b) External torque is applied on the CoM; (c) External force misaligns with the CoM

4.1 External force passing through the CoM

When an external force passes through the CoM, only the initial rest state of the robot will be disturbed while the posture remains upright. In this case, the final state of balance control should recover to the stable orbit and restore the initial upright posture, as described in Eq. (7). For this purpose, we propose an STB primitive for the hip torque. The STB torque primitive is designed as follows:

$$
\tau_{\mathrm{STB}}(t) = \mathrm{sgn}(S_0) \cdot \tau_{\max}\left[1(t) - 2 \cdot 1\left(t - \frac{T}{4}\right) \right.
$$
$$
\left. + 2 \cdot 1\left(t - \frac{3T}{4}\right) - 1(t - T) \right], \tag{14}
$$

where T is the duration of STB control, the sign of the initial torque depends on the sign of initial stable offset S_0 after the disturbances, and the sign of hip torque switches at $T/4$, $3T/4$, and T.

To demonstrate that STB control can restore the initial upright posture, taking $S_0>0$ as an example, we substitute Eq. (14) into Eq. (4) and then integrate the result to obtain the angle and angular velocity of the body from 0 to T, that is,

$$
\begin{bmatrix} \dot{\theta}_{\mathrm{STB}}(t) \\ \theta_{\mathrm{STB}}(t) \end{bmatrix} = \frac{\sigma}{2}\begin{bmatrix} 2t \\ t^2 \end{bmatrix} \cdot 1(t) - \sigma\begin{bmatrix} 2\left(t - \frac{T}{4}\right) \\ \left(t - \frac{T}{4}\right)^2 \end{bmatrix} \cdot 1\left(t - \frac{T}{4}\right)
$$
$$
+ \sigma\begin{bmatrix} 2\left(t - \frac{3T}{4}\right) \\ \left(t - \frac{3T}{4}\right)^2 \end{bmatrix} \cdot 1\left(t - \frac{3T}{4}\right) - \frac{\sigma}{2}\begin{bmatrix} 2(t - T) \\ (t - T)^2 \end{bmatrix} \cdot 1(t - T),
$$

$$\tag{15}$$

where $\sigma = \tau_{\max}/J$, which is also the maximum angular acceleration of the hip joint.

Replacing t in Eq. (15) with duration of STB control T, we find that the angle and angular velocity of the body at T are both 0, which means that the body posture is upright at time T. Based on the definition of the control targets in Eq. (7), if a proper value of T satisfies $S_{\mathrm{STB}}(T)=0$, then STB control is effective.

According to Eq. (3), the horizontal position and velocity of the CoM under STB control at T are

$$\begin{bmatrix} x_{STB}(T) \\ \dot{x}_{STB}(T) \end{bmatrix} = \begin{bmatrix} \cosh(\omega T) & \dfrac{\sinh(\omega T)}{\omega} \\ \omega\sinh(\omega T) & \cosh(\omega T) \end{bmatrix} \begin{bmatrix} x_0 \\ \dot{x}_0 \end{bmatrix}$$

$$+ \begin{bmatrix} \dfrac{\Phi}{\omega}\left[\cosh(\omega T) - 2\cosh\left(\dfrac{3\omega T}{4}\right) + 2\cosh\left(\dfrac{\omega T}{4}\right) - 1\right] \\ \Phi\left[\sinh(\omega T) - 2\sinh\left(\dfrac{3\omega T}{4}\right) + 2\sinh\left(\dfrac{\omega T}{4}\right)\right] \end{bmatrix}.$$

(16)

Substituting Eq. (16) into Eq. (6), the stable offset at T is

$$S_{STB}(T) = S_0 e^{\omega T} - \Phi\left(e^{\omega T} - 2e^{\frac{3\omega T}{4}} + 2e^{\frac{3\omega T}{4}} - 1\right). \quad (17)$$

Since $S_{STB}(0) \cdot S_{STB}(+\infty) < 0$ and $S_{STB}(T)$ is a continuous function of variable T, the solution of $S_{STB}(T) = 0$ ($T \in (0, +\infty)$) must exist. We define the solution as T_{STB}. Using a numerical method, we can obtain the value of T_{STB} within an acceptable time. Replacing T in Eq. (14) with T_{STB}, the hip torque output is determined. STB control can achieve the control targets described in Eq. (7) for all conditions in the case where the disturbance passes through the CoM with the initial stable offset subject to inequality (13) theoretically.

Fig. 3 shows the trajectories of horizontal motion in the phase portrait using STB control, with different T from the initial horizontal motion state (x=0 m, $\dot{x}_0 = -0.15$ m/s) after an impulsive disturbance passes through the CoM. The line formed by the final horizontal motion states intersects with the stable orbit at T=0.496 s. The red curve is the expected trajectory of balance control. Fig. 4 shows five trajectories of balance control using STB control from five different initial horizontal states to their final states in the phase portrait.

4.2 External torque applied to the CoM

When a bipedal robot is standing upright in the rest state, the angle and angular velocity of the body will change in the same direction (θ_0 and $\dot{\theta}_0$ are both increasing or decreasing from 0) after an external torque disturbance is applied, but the initial stable state of the horizontal motion remains unchanged. In this case, a different torque primitive is required for the hip to recover the upright posture without affecting the stable state of the horizontal motion. For this purpose, we propose an ATB primitive for the hip torque. ATB control can also achieve posture recovery when $\theta_0 \neq 0$, $\dot{\theta}_0 = 0$. In other words, any attitude with zero velocity can be recovered.

The ATB torque primitive for the hip is defined as follows:

$$\tau_{ATB}(t) = \mathrm{sgn}(\theta_0) \cdot \tau_{max}\left[1(t) - 2 \cdot 1(t - aT)\right.$$
$$\left. + 2 \cdot 1(t - bT) - 1(t - T)\right], \quad 0 \le a \le b \le 1, \quad (18)$$
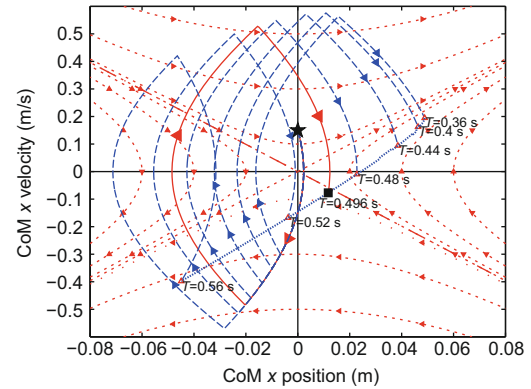

Fig. 3 Trajectories (blue dot curves) of the horizontal motion in the phase portrait with stable orbit (red dot curve) using STB control with different T (0.36–0.56 s) from the initial state of x_0=0 m, $\dot{x}_0 = -0.15$ m/s (pentagram)

The blue coarse dot curve represents the corresponding final states. The red curve is the expected trajectory with T=0.496 s, whose final state is exactly on the stable orbit (m=10 kg, g=9.8 m/s^2, z=0.4 m, τ_{max}=20 N·m). References to color refer to the online version of this figure
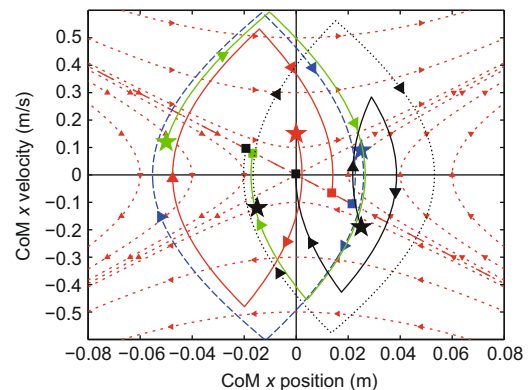

Fig. 4 Five trajectories of the horizontal motion in balance control using STB control from five different initial horizontal motion states (pentagrams) to their final states (rectangles) in the phase portrait

where T is the duration of ATB control, and the value of the torque switches at aT, bT, and T. The sign of the starting torque depends on the sign of the initial angle.

Taking the case of $\theta_0>0$ and $\dot{\theta}_0 > 0$ as an example, given the hip torque of Eq. (18), the angle and angular velocity of the body at T are

$$\begin{bmatrix} \dot{\theta}_d \\ \theta_d \end{bmatrix} = \begin{bmatrix} 1 & 0 \\ T & 1 \end{bmatrix} \begin{bmatrix} \dot{\theta}_0 \\ \theta_0 \end{bmatrix} + \frac{\sigma T^2}{2} \begin{bmatrix} (4a-4b+2)/T \\ -2a^2+2b^2+4a-4b+1 \end{bmatrix},$$
(19)

where θ_d and $\dot{\theta}_d$ are the desired angle and angular velocity of the body, respectively. They are both 0 in the particular case of keeping an upright posture.

Substituting θ_d and $\dot{\theta}_d$ into Eq. (19), a and b are written as

$$\begin{cases} a = -\dfrac{N}{2M} - \dfrac{M}{2} + 1, \\ b = -\dfrac{N}{2M} + \dfrac{M}{2} + 1, \end{cases}$$
(20)

where $M = \dfrac{1}{2} + \dfrac{\dot{\theta}_0}{2\sigma T}$ and $N = \dfrac{1}{2} + \dfrac{\theta_0 + \dot{\theta}_0 T}{\sigma T^2}$. Given the constraint $a \geq 0$, there is

$$-\frac{N}{2M} - \frac{M}{2} + 1 \geq 0.$$
(21)

Substituting M and N into inequality (21) yields

$$\left(T - \frac{\dot{\theta}_0}{\sigma}\right)^2 \geq \frac{4\sigma\theta_0 + 2\dot{\theta}_0^2}{\sigma^2}.$$
(22)

Since the minimum time for the initial angular velocity $\dot{\theta}_0$ to reduce to 0 is $\dot{\theta}_0 / \sigma$, the duration T must satisfy $T \geq \dot{\theta}_0 / \sigma$. Solving inequality (22), we obtain the inequality constraint of T as

$$T \geq \frac{\dot{\theta}_0 + \sqrt{4\sigma\dot{\theta}_0 + 2\dot{\theta}_0^2}}{\sigma}.$$
(23)

The minimum value of T is

$$T_{min} = \frac{\dot{\theta}_0 + \sqrt{4\sigma\dot{\theta}_0 + 2\dot{\theta}_0^2}}{\sigma},$$
(24)

and the values of a and b corresponding to T_{min} are

$$\begin{cases} a = 0, \\ b = \lambda, \end{cases}$$
(25)

where

$$\lambda = \frac{\dot{\theta}_0 + \sqrt{4\sigma\theta_0 + 2\dot{\theta}_0^2}}{\dot{\theta}_0 + 2\sqrt{4\sigma\theta_0 + 2\dot{\theta}_0^2}}.$$
(26)

In fact, the ATB primitive is actually a bang-bang profile when $T=T_{min}$.

As for the case of $\theta_0<0$ and $\dot{\theta}_0 < 0$, we also obtain

$$T_{min} = \frac{-\dot{\theta}_0 + \sqrt{-4\sigma\theta_0 + 2\dot{\theta}_0^2}}{\sigma}.$$
(27)

The values of a and b corresponding to T_{min} in Eq. (27) also satisfy Eq. (25).

Observing Eqs. (24) and (27), in either case, we have

$$T_{min} = \frac{|\dot{\theta}_0| + \sqrt{4\sigma|\theta_0| + 2\dot{\theta}_0^2}}{\sigma}.$$
(28)

From Eq. (20), we draw the conclusion that the difference between the total duration of the positive torque and that of the negative torque, $D_{diff}=(aT+T-bT)-(bT-aT)=T(1+2a-2b)=T(1-2M)=\dot{\theta}_0/(2\sigma)$, is dependent only on $\dot{\theta}_0$, which means D_{diff} is determined by the initial angular velocity of body in ATB control. In the case of $\dot{\theta}_0 = 0$, we have $D_{diff}=0$. So, the total duration of the positive torque is equal to that of the negative value, as described in Section 4.1. In more generic cases, at a certain duration of ATB control T, the parameters of ATB control, a and b, can be uniquely identified by the requirement of θ_d and $\dot{\theta}_d$. Based on the definition of the control targets in Eq. (7), if a proper duration of ATB control $T \in [T_{min}, +\infty)$ satisfies $S_{ATB}(T)=0$, then ATB control is effective.

Under the ATB control in Eq. (18), the horizontal position and velocity of the CoM at T are

$$\begin{bmatrix} x_{\mathrm{ATB}}(T) \\ \dot{x}_{\mathrm{ATB}}(T) \end{bmatrix} =$$

$$\frac{\varPhi}{\omega} \begin{bmatrix} \cosh(\omega T) - 2\cosh((1-a)\omega T) + 2\cosh((1-b)\omega T) - 1 \\ k\sinh(\omega T) - 2k\sinh((1-a)\omega T) + 2k\sinh((1-b)\omega T) \end{bmatrix}.$$
(29)

Substituting Eq. (29) into Eq. (6), the stable offset at T is

$$S_{\mathrm{ATB}}(T) = -\varPhi[\mathrm{e}^{\omega T} - 2\mathrm{e}^{(1-a)\omega T} + 2\mathrm{e}^{(1-b)\omega T} - 1]. \quad (30)$$

According to Eqs. (25) and (30), the stable offset at $T_{\min}$ is

$$S_{\mathrm{ATB}}(T_{\min}) = \varPhi[\mathrm{e}^{\omega T_{\min}} + 1 - 2\mathrm{e}^{(1-\lambda)\omega T_{\min}}]. \quad (31)$$

From Eq. (31), given $1-\lambda<0.5$, $S_{\mathrm{ATB}}(T_{\min})>0$. In addition, $S_{\mathrm{ATB}}(+\infty)<0$. Since $S_{\mathrm{ATB}}(T)$ is a continuous function of variable T, the solution of $S_{\mathrm{ATB}}(T)=0$ ($T\in[T_{\min}, +\infty)$) exists. We name it T_{ATB}. The value of T_{ATB} can be calculated via the numerical approach.

Fig. 5a shows the trajectories of ATB control from the initial posture ($\theta_0=0$ rad, $\dot{\theta}_0=1$ rad/s) with different T in the phase portrait. The line formed by final states (blue coarse dot curve) intersects with the stable orbit (red dot curve) at $T=0.658$ s. The red curve is the expected trajectory of the upright posture

recovery. Fig. 5b shows the curves of the ATB hip torque primitive (top), angular velocity (middle), and angle (bottom) of the body. The error in the angle of the body can be compensated by ATB control without affecting balance.

4.3 External force misaligning with the CoM

In most cases, external forces applied on the body rarely pass through the CoM or solely produce a torque around the CoM. Such disturbances will change the horizontal motion and body posture at the same time. It is more realistic to deal with such realistic external disturbances, simultaneously restoring the balance and posture using the hip strategy.

According to the applied position of external forces and the initial horizontal motion and body posture after the perturbations, external perturbations are divided into eight types (Table 1). Based on the discussions in Sections 4.1 and 4.2, STB and ATB control can be formulated using a sign function to determine the initial polarity of output and thus an adaptive bang-bang-bang function. To deal with all types of external disturbances, a specialized sign function, decided by not only the initial posture but also the relationship between initial horizontal motion and initial posture, is designed to determine the initial sign of the torque. We propose a UTB control for the hip torque, similar to Eq. (18), which can recover
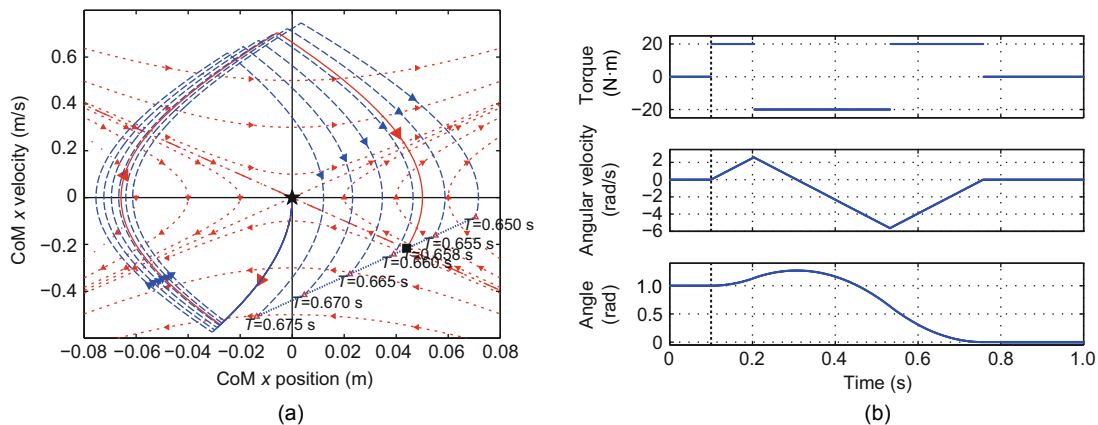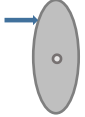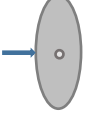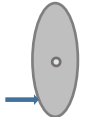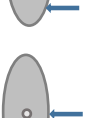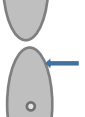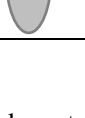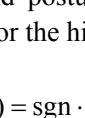

Fig. 5 Trajectories (blue dot curves) of the horizontal motion in the phase portrait with stable orbit (red dot curve) using ATB control with different duration T (0.650–0.675 s) from the initial state of $x_0=0$ m, $\dot{x}_0=0$ m/s and posture of $\theta_0=0$ rad, $\dot{\theta}_0=1$ rad/s (a) and the curves of the ATB torque primitive for the hip with $T=0.658$ s (top), the angular velocity (middle), and angle (bottom) of the body (b)

In (a), the blue coarse dot curve represents the corresponding final states and the red curve is the expected trajectory with $T=0.658$ s, whose final state is exactly on the stable orbit. Pentagrams represent each initial value and rectangles represent each final value ($J=0.8$ kg·m²). References to color refer to the online version of this figure

Table 1 Eight cases of external force perturbations

Case	Acting position	Initial horizontal motion	Initial body posture	sgn	a and b corresponding to T_{min}
1		$\begin{cases} x_0 > 0 \\ \dot{x}_0 > 0 \end{cases}$	$\begin{cases} \theta_0 \geq 0 \\ \dot{\theta}_0 \geq 0 \end{cases}$	+1	$\begin{cases} a = 0 \\ b = \lambda \end{cases}$
2		$\begin{cases} x_0 > 0 \\ \dot{x}_0 > 0 \end{cases}$	$\begin{cases} \theta_0 = 0 \\ \dot{\theta}_0 = 0 \end{cases}$	+1	$\begin{cases} a = 0 \\ b = \lambda \end{cases}$
3		$\begin{cases} x_0 > 0 \\ \dot{x}_0 > 0 \end{cases}$	$\begin{cases} \theta_0 < 0 \\ \dot{\theta}_0 < 0 \end{cases}$	+1: $S_0 \geq -\Phi[1-2\exp(-\omega\lambda T_{min})+\exp(-\omega T_{min})]$	$\begin{cases} a = 0 \\ b = \lambda \end{cases}$
4				-1: $S_0 < -\Phi[1-2\exp(-\omega\lambda T_{min})+\exp(-\omega T_{min})]$	$\begin{cases} a = \lambda \\ b = 1 \end{cases}$
5		$\begin{cases} x_0 < 0 \\ \dot{x}_0 < 0 \end{cases}$	$\begin{cases} \theta_0 > 0 \\ \dot{\theta}_0 > 0 \end{cases}$	+1: $S_0 > \Phi[1-2\exp(-\omega\lambda T_{min})+\exp(-\omega T_{min})]$	$\begin{cases} a = \lambda \\ b = 1 \end{cases}$
6				-1: $S_0 \leq \Phi[1-2\exp(-\omega\lambda T_{min})+\exp(-\omega T_{min})]$	$\begin{cases} a = 0 \\ b = \lambda \end{cases}$
7		$\begin{cases} x_0 < 0 \\ \dot{x}_0 < 0 \end{cases}$	$\begin{cases} \theta_0 = 0 \\ \dot{\theta}_0 = 0 \end{cases}$	-1	$\begin{cases} a = 0 \\ b = \lambda \end{cases}$
8		$\begin{cases} x_0 < 0 \\ \dot{x}_0 < 0 \end{cases}$	$\begin{cases} \theta_0 < 0 \\ \dot{\theta}_0 < 0 \end{cases}$	-1	$\begin{cases} a = 0 \\ b = \lambda \end{cases}$

balance and posture in all cases. The UTB torque primitive for the hip is defined as follows:

$$\tau_{UTB}(t) = sgn \cdot \tau_{max} \left[1(t) - 2 \cdot 1(t - aT) + 2 \cdot 1(t - bT) - 1(t - T) \right], \quad 0 \leq a \leq b \leq 1, \tag{32}$$

where the value of sgn can be found in Table 1.

Recalling the calculation of the minimum value of T in Section 4.2, the minimum duration of UTB control of the constraint $a \geq 0$ still satisfies Eq. (28), whether or not the external disturbance is any of the cases in Table 1. Note that the values of a and b corresponding to T_{min} do not satisfy Eq. (25), but their particular values can be retrieved from the last column in Table 1.

When the external perturbation is case 3 (Table 1), we have sgn=1. Under the UTB control in Eq. (32), the horizontal position and velocity of the CoM at T are

$$\begin{bmatrix} x_{UTB}(T) \\ \dot{x}_{UTB}(T) \end{bmatrix} = \begin{bmatrix} \cosh(\omega T) & \dfrac{\sinh(\omega T)}{\omega} \\ \omega\sinh(\omega T) & \cosh(\omega T) \end{bmatrix} \begin{bmatrix} x_0 \\ \dot{x}_0 \end{bmatrix} + \begin{bmatrix} \dfrac{\Phi[\cosh(\omega T)-2\cosh((1-a)\omega T)+2\cosh((1-b)\omega T)-1]}{\omega} \\ \Phi[\sinh(\omega T)-2\sinh((1-a)\omega T)+2\sinh((1-a)\omega T)] \end{bmatrix}. \tag{33}$$

Substituting Eq. (33) into Eq. (6), the stable offset at T is

$$S_{UTB}(T) = S_0 e^{\omega T} - \Phi[e^{\omega T} - 2e^{(1-a)\omega T} + 2e^{(1-b)\omega T} - 1]. \tag{34}$$

Setting $T = T_{min}$, we have

$$S_{UTB}(T_{min}) = S_0 e^{\omega T_{min}} + \Phi[e^{\omega T_{min}} + 1 - 2e^{(1-\lambda)\omega T_{min}}]. \tag{35}$$

In this case, $S_{UTB}(T_{min}) \geq 0$ is definite given $S_0 \geq -\Phi(1 - 2e^{-\omega\lambda T_{min}} + e^{-\omega T_{min}})$. Meanwhile, $S_{UTB}(+\infty)=$

$(S_0-\Phi)\mathrm{e}^{+\omega\infty}<0$ when $T=+\infty$. Because $S_{\mathrm{UTB}}(T)$ is a continuous function of variable T, a proper value of T must exist to satisfy $S_{\mathrm{UTB}}(T)=0$, and thus UTB control is effective.

When the external perturbation is case 4, we have sgn$=-1$. Under UTB control in Eq. (32), the horizontal position and velocity of the CoM at T are

$$\begin{bmatrix} x_{\mathrm{UTB}}(T) \\ \dot{x}_{\mathrm{UTB}}(T) \end{bmatrix} = \begin{bmatrix} \cosh(\omega T) & \dfrac{\sinh(\omega T)}{\omega} \\ \omega\sinh(\omega T) & \cosh(\omega T) \end{bmatrix}\begin{bmatrix} x_0 \\ \dot{x}_0 \end{bmatrix}$$
$$-\begin{bmatrix} \dfrac{\Phi[\cosh(\omega T)-2\cosh((1-a)\omega T)+2\cosh((1-b)\omega T)-1]}{\omega} \\ \Phi[\sinh(\omega T)-2\sinh((1-a)\omega T)+2\sinh((1-b)\omega T)] \end{bmatrix}.$$
(36)

Substituting Eq. (36) into Eq. (6), the stable offset at T is

$$S_{\mathrm{UTB}}(T) = S_0\mathrm{e}^{\omega T} + \Phi[\mathrm{e}^{\omega T} - 2\mathrm{e}^{(1-a)\omega T} + 2\mathrm{e}^{(1-b)\omega T} - 1].$$
(37)

When $T=T_{\min}$, we have

$$S_{\mathrm{UTB}}(T_{\min}) = S_0\mathrm{e}^{\omega T_{\min}} + \Phi[\mathrm{e}^{\omega T_{\min}} - 2\mathrm{e}^{(1-\lambda)\omega T_{\min}} + 1]. \quad (38)$$

Given $S_0 < -\Phi(1 - 2\mathrm{e}^{-\omega\lambda T_{\min}} + \mathrm{e}^{-\omega T_{\min}})$, we obtain $S_{\mathrm{UTB}}(T_{\min})<0$. Meanwhile, $S_{\mathrm{UTB}}(+\infty)= (S_0+\Phi)\mathrm{e}^{+\omega\infty}>0$ when $T=+\infty$. A suitable value of T must exist to satisfy $S_{\mathrm{UTB}}(T)=0$.

When the external perturbation is case 1, 6, or 8, UTB control can be proved effective by referring to case 3. Then it is also applicable for case 5 by referring to case 4. Cases 2 and 7 can be referred to the STB control in Section 4.1. In summary, UTB control can achieve balance control and posture recovery simultaneously, regardless of the type of external force.

Fig. 6a shows the six trajectories of balance control and posture recovery using UTB control starting from six different initial states to the final states in the phase portrait. Fig. 6b shows the corresponding six datasets of the UTB hip torque primitive (top), angular velocity (middle), and angle (bottom) of the body. The errors in the angular position and velocity of the body can be reduced to zero by UTB control.
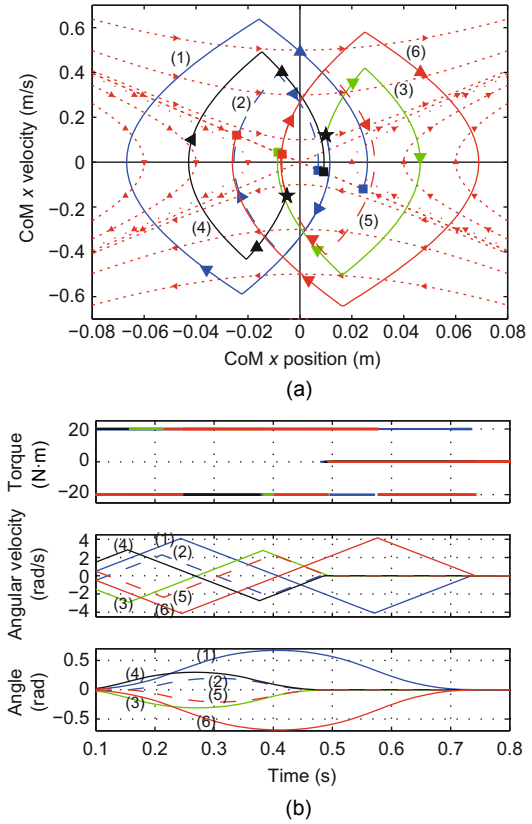

Fig. 6 Six trajectories of the horizontal motion in balance control using UTB control from six different initial horizontal motion states (pentagrams) to their final states (rectangles) respectively in the phase portrait (a) and the six corresponding data of the UTB torque primitive for the hip (top), angular velocity (middle), and angle (bottom) of the body (b)

Six different initial states $(x_0, \dot{x}_0, \theta_0, \dot{\theta}_0)$ are (0.01, 0.12, 0.01, 0.5), (0.01, 0.12, −0.01, −0.5), (0.01, 0.12, −0.02, −1.5), (−0.005, −0.15, 0.02, 1.5), (−0.005, −0.15, 0.01, 0.5), (−0.005, −0.15, −0.01, −0.5), respectively

5 Simulation results

Simulations have been conducted on a bipedal robot with four degrees of freedom. The body of the robot is located at the hip joint with mass of m=20 kg and inertia of J=1.6 kg·m^2. The mass of each leg is 0.9 kg and the maximum hip torque is $\tau_{\max}$=20 N·m. To avoid lateral movement, the single support phase is set up by standing with the two legs side by side at the same horizontal position. The weight of the robot is equally distributed on each leg. The desired height of the CoM is 0.4 m in the simulation.

5.1 Simulation of STB control

Fig. 7 shows a sequence of time-elapsed images of the bipedal robot using STB control after an impulsive disturbance which changes the horizontal position from 0 to 0.005 m and the velocity from 0 to 0.2 m/s. Fig. 8a shows the trajectory of the corresponding horizontal motion in the phase portrait. Fig. 8b shows the corresponding torque primitive for the hip, and the angular velocity and angle of the body. Note that the control of the upper body posture is included in the STB method, which can be seen by the convergence of the body posture back to the initial upright posture. The standing balance is successfully achieved by STB control with the regulation of the upright posture at the same time.
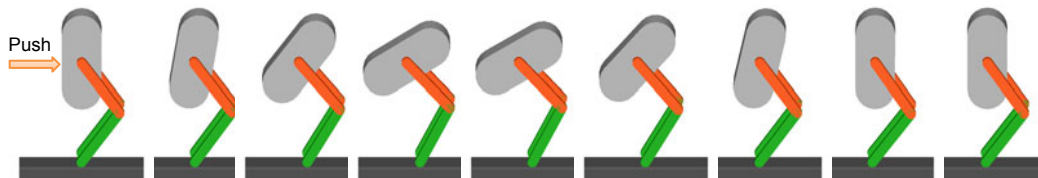
5.2 Simulation of ATB control

Fig. 9 shows the time-elapsed snapshots of the biped using ATB control to recover the body posture from 0.75 to 0 rad without affecting the balance in horizontal motion.

Fig. 10a shows the trajectory of the corresponding horizontal motion in the phase portrait. Fig. 10b shows the corresponding torque primitive for the hip, and the angular velocity and angle of the body. The posture recovery is achieved with the initial body pitch of 0.75 rad without affecting the standing balance.

5.3 Simulation of UTB control

Fig. 11 shows the time-elapsed snapshots of the simulated biped using UTB control after an

Fig. 7 Time-elapsed snapshots from dynamic simulation where the simulated biped recovers from an impulsive disturbance using STB control (snapshots are sequenced from left to right at a 0.08 s interval)
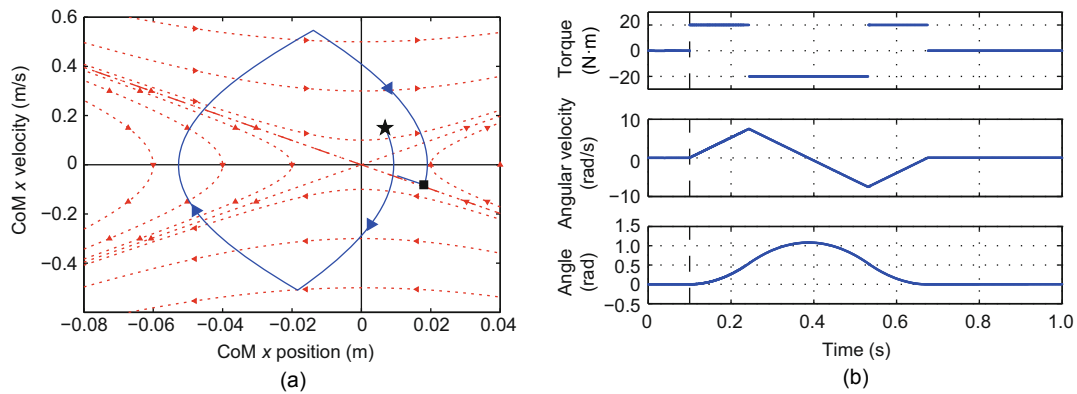

Fig. 8 The phase portrait of the horizontal motion, corresponding to Fig. 7, showing the responses under STB control (a) and simulation data corresponding to Fig. 7 (b)
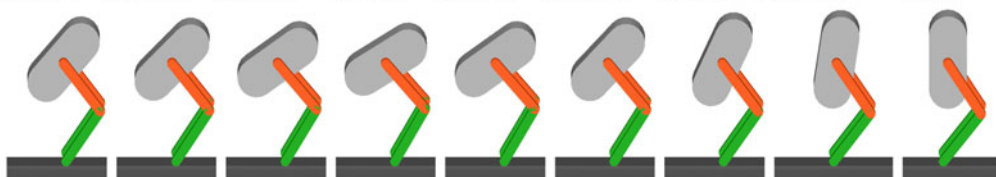

Fig. 9 Time-elapsed snapshots which show that the simulated biped recovers posture from 0.75 to 0 rad using ATB control (snapshots are sequenced from left to right at a 0.05 s interval)

impulsive disturbance which perturbs the horizontal position from 0 to 0.005 m, the velocity from 0 to 0.2 m/s, and the angular velocity of the body from 0 to 0.5 rad/s.

Fig. 12a shows the trajectory of the corresponding horizontal motion in the phase portrait. Fig. 12b shows the corresponding torque primitive for the hip, the angular velocity, and the angle of the body. Balance control and posture recovery are both completed using UTB control.

5.4 Simulation of LQR control

To prove that the advantage of the open-loop methods of torque primitives lies in rapid response and reasonable performance, a comparison simulation has been made using LQR control with the same initial conditions. According to Eqs. (3) and (4), and setting x, $\dot{x}$, , θ_b, and $\dot{\theta}_b$ as the state variables and τ_h the only control variable, the state equation of the body is
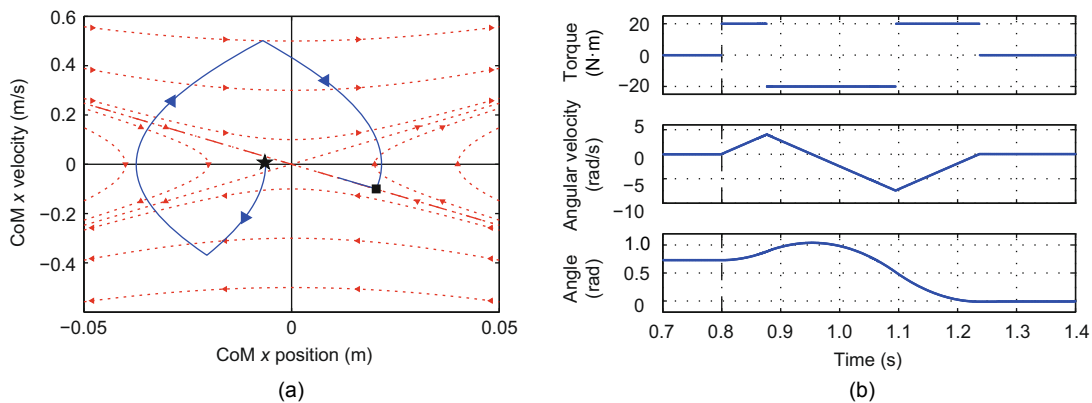

Fig. 10 The phase portrait of the horizontal motion, corresponding to Fig. 9, showing the responses under ATB control (the initial and final states are both in the stable orbit) (a) and simulation data corresponding to Fig. 9 (b)
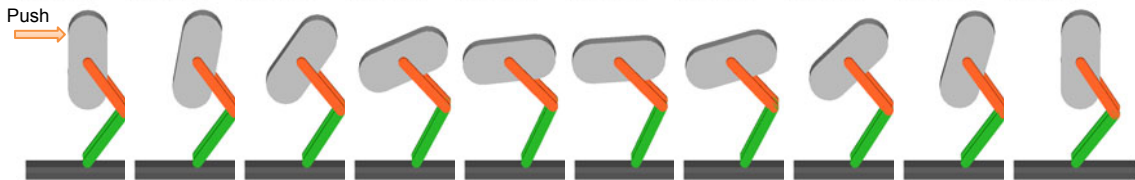

Fig. 11 Time-elapsed snapshots showing that the simulated robot recovers from an impulsive disturbance by UTB control (snapshots are sequenced from left to right at a 0.08 s interval)
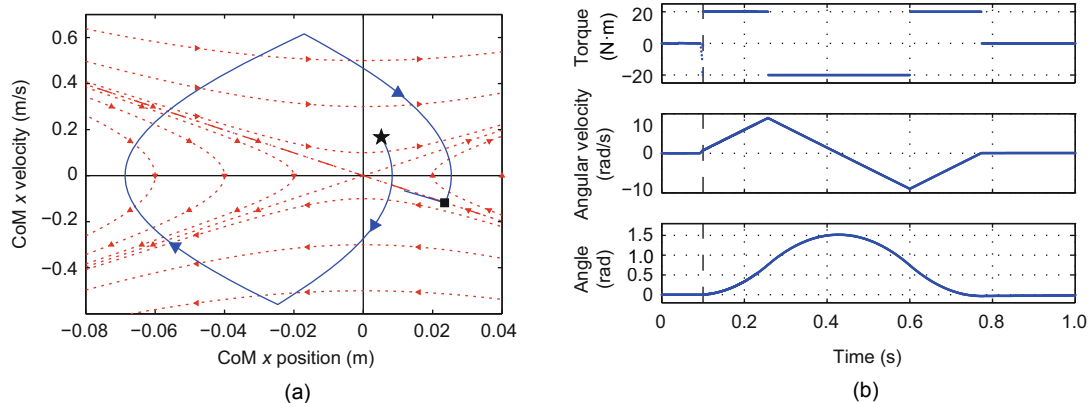

Fig. 12 The trajectory of the horizontal motion in the phase portrait, corresponding to Fig. 11, showing the responses under UTB control (a) and simulation data corresponding to Fig. 11 (b)

$$\begin{bmatrix} \dot{x} \\ \ddot{x} \\ \dot{\theta}_b \\ \ddot{\theta}_b \end{bmatrix} = \begin{bmatrix} 0 & 1 & 0 & 0 \\ \omega^2 & 0 & 0 & 0 \\ 0 & 0 & 0 & 1 \\ 0 & 0 & 0 & 0 \end{bmatrix} \begin{bmatrix} x \\ \dot{x} \\ \theta_b \\ \dot{\theta}_b \end{bmatrix} + \begin{bmatrix} 0 \\ -1/(zm) \\ 0 \\ 1/J \end{bmatrix} \tau_h. \quad (39)$$

The standing under-actuated biped is a time-invariant continuous system. From Eq. (39), the LQR method is suitable when the initial stable offset is less than Φ and the kinematics and friction angle constraints are also satisfied. Then a comparison simulation using LQR control with optimized parameters is conducted. Fig. 13a shows the trajectory of the horizontal motion under LQR control in the phase portrait. Fig. 13b shows the corresponding hip torque, the angular velocity, and the angle of the body. Comparing Figs. 12 and 13, we find that the open-loop methods of torque primitives can recover both balance and body posture faster.
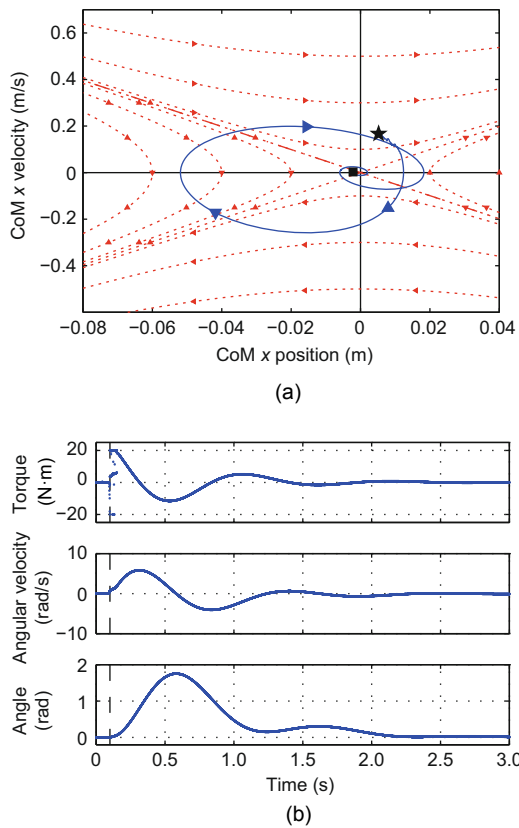

(a)

(b)

Fig. 13 The trajectory of the horizontal motion in the phase portrait, showing the responses from LQR control (a) and the corresponding simulation data (b)

6 Conclusions and future work

In this paper, three different hip strategies were proposed for simultaneously controlling the standing balance and body posture under different impulsive force disturbances on bipedal robots. The proposed STB control can achieve balance control without changing the initial upright posture of the body, and ATB control was proposed for modifying the posture error without losing balance in the horizontal motion. Finally, UTB control was designed for simultaneously recovering the balance and regulating the body orientation. The simulation study of a simplified bipedal robot has been carried out to demonstrate the effectiveness of our proposed controllers. In addition, more types of torque primitives (e.g., cosine and cubic spline) have been tested to complete both balance control and posture recovery. However, the bang-bang-bang control is still the fastest.

The ongoing work involves taking into account the limits of the angle and angular velocity of the body, and the condition of slipping, and designing a more general torque primitive for the hip to achieve balance control and posture recovery at more complicated initial states of the horizontal motion and body posture after an impulsive disturbance as well as with a continuous disturbance.

Moreover, a small trial research and investigation in push recovery for the biped with the hip joint being not located at the CoM, has been carried out. Our method has a certain effect in cases where the hip joint and the CoM are close, but is not very effective when they are relatively far from each other. In the latter situation, the knee joints regularly come close to or even reach the singular position when the body has a large pitch angle. The most important reason is that the CoM height must be retained due to the LIPM being adopted. For those cases, standing push recovery based on the double inverted pendulum or some other models should be a better solution. However, the method in this paper would be effective for the planar bipedal robots with hip joints both located close to the CoM, which are currently being developed in our laboratory.

As for future work, a series of real experiments will be carried out on the planar bipedal robot with the series elastic actuator (SEA) joints. The SEA joints will provide the torque control capability which

allows us to validate our proposed hip strategies using the torque primitives.

References

Ahmed, S.M., Chew, C.M., Tian, B., 2013. Standing posture modeling and control for a humanoid robot. Proc. IEEE/RSJ Int. Conf. on Intelligent Robots and Systems, p.4152-4157. [doi:10.1109/IROS.2013.6696951]

Azevedo, C., Espiau, B., Amblard, B., *et al.*, 2007. Bipedal locomotion: toward unified concepts in robotics and neuroscience. *Biol. Cybern.*, **96**(2):209-228. [doi:10.1007/s00422-006-0118-0]

Horak, F.B., Nashner, L.M., 1986. Central programming of postural movements: adaptation to altered support-surface configurations. *J. Neurophysiol.*, **55**(6):1369-1381.

Hyon, S., Hale, J.G., Cheng, G., 2007. Full-body compliant human-humanoid interaction: balancing in the presence of unknown external forces. *IEEE Trans. Robot.*, **23**(5):884-898. [doi:10.1109/TRO.2007.904896]

Kajita, S., Tani, K., 1991. Study of dynamic biped locomotion on rugged terrain-derivation and application of the linear inverted pendulum mode. Proc. IEEE Int. Conf. on Robotics and Automation, p.1405-1411. [doi:10.1109/ROBOT.1991.131811]

Lee, S.H., Goswami, A., 2010. Ground reaction force control at each foot: a momentum-based humanoid balance controller for non-level and non-stationary ground. Proc. IEEE/RSJ Int. Conf. on Intelligent Robots and Systems, p.3157-3162. [doi:10.1109/IROS.2010.5650416]

Li, Z., Vanderborght, B., Tsagarakis, N.G., *et al.*, 2012. Stabilization for the compliant humanoid robot COMAN exploiting intrinsic and controlled compliance. Proc. IEEE Int. Conf. on Robotics and Automation, p.2000-2006. [doi:10.1109/ICRA.2012.6224705]

Liu, C., Atkeson, C.G., 2009. Standing balance control using a trajectory library. Proc. IEEE/RSJ Int. Conf. on Intelligent Robots and Systems, p.3031-3036. [doi:10.1109/IROS.2009.5354018]

Orin, D.E., Goswami, A., Lee, S.H., 2013. Centroidal dynamics of a humanoid robot. *Auton. Robots*, **35**(2-3):161-176. [doi:10.1007/s10514-013-9341-4]

Pratt, J., Carff, J., Drakunov, S., *et al.*, 2006. Capture point: a step toward humanoid push recovery. Proc. IEEE-RAS Int. Conf. on Intelligent Robots, p.200-207. [doi:10.1109/ICHR.2006.321385]

Runge, C.F., Shupert, C.L., Horak, F.B., *et al.*, 1999. Ankle and hip postural strategies defined by joint torques. *Gait Post.*, **10**(2):161-170. [doi:10.1016/S0966-6362(99)00032-6]

Spong, M., 1995. The swing up control problem for the acrobat. *IEEE Contr. Syst.*, **15**(1):49-55. [doi:10.1109/37.341864]

Stephens, B., 2007a. Humanoid push recovery. Proc. IEEE-RAS Int. Conf. on Humanoid Robots, p.589-595. [doi:10.1109/ICHR.2007.4813931]

Stephens, B., 2007b. Integral control of humanoid balance. Proc. IEEE/RSJ Int. Conf. on Intelligent Robots and Systems, p.4020-4027. [doi:10.1109/IROS.2007.4399407]

Stephens, B., Atkeson, C.G., 2010. Dynamic balance force control for compliant humanoid robots. Proc. IEEE/RSJ Int. Conf. on Intelligent Robots and Systems, p.1248-1255. [doi:10.1109/IROS.2010.5648837]

Wang, J., 2012. Humanoid push recovery with robust convex synthesis. Proc. IEEE/RSJ Int. Conf. on Intelligent Robots and Systems, p.4354-4359. [doi:10.1109/IROS.2012.6386211]

Wang, Y., Xiong, R., Zhu, Q., *et al.*, 2014. Compliance control for standing maintenance of humanoid robots under unknown external disturbances. Proc. IEEE Int. Conf. on Robotics and Automation, p.2297-2304. [doi:10.1109/ICRA.2014.6907177]

Whitman, E.C., Stephens, B.J., Atkeson, C.G., 2012. Torso rotation for push recovery using a simple change of variables. Proc. IEEE-RAS Int. Conf. on Humanoid Robots, p.50-56. [doi:10.1109/HUMANOIDS.2012.6651498]